STM JOURNALS

Journal of
Thermal Engineering and Applications

ISSN: 2349-8994
Volume 11, Issue 2, 2024
May–August
DOI (Journal): 10.37591/JoTEA

https://journals.stmjournals.com/jotea

Research JoTEA

Cogeneration System in Concentrated Photovoltaic Panels

Carlos Armenta-Deu*

Abstract

This study analyzes the behavior of hybrid systems composed of photovoltaic (PV) panels and phase-change materials (PCMs) under solar concentration conditions, aiming to generate electric and thermal energy in water simultaneously (cogeneration). This work looks for system performance improvement while increasing the generated power and energy by the PV panel and the thermal system in unison. The study shows the increase in power and energy delivered by the prototype compared to the power supply by conventional configuration without solar concentration. Likewise, the work evaluates the PV panel's electric energy efficiency and the thermal system performance as a single and combined system. The hybrid PV-PCM-heat exchanger system operates in high-efficiency mode, with typical performance up to 2.1 times higher for the PV panel and 107% more global energy generation. The hybrid system coefficient of performance (COP) evolves from a minimum of 1.017 for standard solar concentration ratio (C_x = 1) to a maximum of 1.283 for C_x = 3.0; the COP value may rise to 3.5 for solar concentration ratio of 20, matching the performance of the highest efficiency conversion systems.

Keywords: Electric and thermal energy cogeneration, hybrid energy generation system photovoltaic–phase change material (PCM)–heat exchange device, efficiency improvement, coefficient of performance

INTRODUCTION

Within the broad field of renewable energies, many justified criticisms arise today, mainly the low energy density they have compared to energy sources of fossil origin [1–3]. We can mention the considerable number of wind turbines required and the surface area necessary to generate the same power as a conventional thermal plant. Various environmental groups are against this type of technology because of the wildland amount they can occupy and the impact on animals and the environment [4–7]. Solar photovoltaic (PV) panels can also represent an impact on wildlife, but there are already efforts to mitigate it at low levels [8–12].

Another characteristic problem of renewable energies is their intermittency. It is not necessary to have meteorological knowledge to know that a wind farm cannot produce at any power level if there are no strong winds, a solar power plant does not generate electricity at night, and hydroelectric power plants do not generate power if there is a drought or low water level [13–16]. Supply based on dependent sources of resources whose availability is beyond human control means less reliability than conventional sources; this is why larger hydroelectric plants work with reservoirs and pumping systems, wind farms base their production on annual percentages of nominal power, and solar thermal plants use large storage tanks [17–20].

A disadvantage of PV systems, which do not exist in the rest of the renewable energies, is their increase in temperature [21–23]. Due to its inherent exposure to sunlight, the temperature on its surface

***Author for Correspondence**
Carlos Armenta-Deu
E-mail: cardeu@fis.ucm.es

Faculty, Department of Physics, Complutense University, Madrid, Spain

Received Date: July 12, 2024
Accepted Date: July 16, 2024
Published Date: July 30, 2024

Citation: Carlos Armenta-Deu. Cogeneration System in Concentrated Photovoltaic Panels. Journal of Thermal Engineering and Applications. 2024; 11(2): 1–14p.

can easily exceed 70°C [24]. It is a well-known fact in the field of renewable energies that PV panels work in optimal conditions at the nominal operating temperature of cell (NOTC) point, which is usually the standard ambient temperature of 20°C [25]. If the temperature increases, the panel efficiency gradually decreases due to the complexity of its electronic components and the properties of its semiconductor materials, representing significant losses regarding the total daily production [21, 26–28].

PV panel efficiency drop is due to the voltage dependence on temperature [29]. Experimental tests show that voltage is inversely proportional to temperature. When the temperature of a PV cell increases, the current-voltage curve of that cell denotes a drastic drop in the maximum voltage, resulting in a decrease in the maximum power point. Although the current shows the opposite effect, increasing proportionally to the temperature, the gain is too small to compensate for the voltage losses [30].

Within the experimental field of PV technologies, cooling methods for the panels look to maintain constant and low temperatures to prevent losses such as water cooling, the most accessible and least polluting refrigerant [31–38]. However, they usually require high investment costs and involve large consumption of water resources. Another cooling medium for PV panels is thermal dissipation tapes, although they are in limited development [39, 40].

A technology with higher development at an experimental level is phase-change materials (PCMs). These substances are of the paraffin family, whose melting point is close to the temperature values reached by the PV cells during the day [41]. Containers filled with these are installed under the solar collectors to absorb the heat accumulated on their surfaces through conduction. When paraffin changes state, its absorption capacity increases significantly due to the latent heat. Likewise, thanks to how easy it is to reverse their state when applying external thermal energy sources, PCMs are considered popular thermal energy storage media [42].

Regarding thermal storage capacity, PCMs are valid as refrigerants and heat sources for different processes [43–45]. Among others, food processing, pharmaceutical, and textile industries require hot water for process development. Using wasted heat that harms PV production as an additional renewable resource is an opportunity that merits detailed study. The heat flow from polluting sources such as diesel or coal would instead come from a zero-emission and unlimited source such as solar energy [46, 47].

Heat recovery systems always require two inlets and outlets where both fluids present in the exchange of thermal energy interact through convection and conduction without coming into contact [48, 49]. Nevertheless, in PCM systems, the mechanism is less complex than in flat plate or tube shell configurations. The water cycle to be heated would pass through a duct that would cross the paraffin container without coming into contact with them so that it simultaneously serves as their coolant [50–52].

FUNDAMENTALS

Solar Concentration

The solar radiation level on the Earth's surface depends on weather conditions, which reduces the extraterrestrial intensity to a lower value. Since solar radiation absorption depends on the atmospheric particle composition and concentration, the surface intensity is variable; therefore, the solar radiation international community adopts an average value of 1000 W/m^2, known as the solar constant, equivalent to one Sun [53].

Nevertheless, thanks to light concentration technologies, we may increase the light incident on a surface above the solar constant value (Sun). Solar thermal plants use large reflecting surfaces, whether parabolic troughs or large mirrors, pointing at a target with a smaller surface area to drastically increase the temperature of their heat transfer fluid. On the other hand, concentrated PV solar panels use magnifying lenses and curved mirrors on the photovoltaic surface to produce the same or more than a conventional PV panel [54].

The following equations show the effects of concentrated solar radiation on the characteristic parameters of a photovoltaic cell or panel [55]:

$$I_{SC}(C) = CI_{SC} \tag{1}$$

$$V_{OC}(C) = V_{OC} + \frac{k_B T}{q}\ln C \tag{2}$$

$$FF = \frac{V_{OC} - \frac{k_B T}{q}\ln\left(\frac{qV_{OC}}{k_B T} + 0.72\right)}{V_{OC} + \frac{k_B T}{q}} \tag{3}$$

$$\eta(C) = \eta_o\left[\frac{FF(C)}{FF_o}\right]\left[1 + \frac{k_B T \ln C}{V_{OC}}\right] \tag{4}$$

where I_{SC} and V_{OC} are the short circuit current and open circuit voltage, k_B is the Boltzmann constant, T is the Kelvin temperature, q is the electron charge, FF is the fill factor, η is the efficiency, and C is the solar concentration ratio.

Heat Transfer

In a hybrid system consisting of a PV panel, a PCM device, and a heat exchanger, the heat transfer process occurs by conduction. Although there are quite a few formulas for calculating the energy transmitted by conduction based on the geometry of the system, the general formula takes the following form (Fourier's law) [56]:

$$\dot{Q}_{cd} = -\kappa A\frac{\partial T}{\partial x} \tag{5}$$

If we deal with finite instead of infinitesimal elements:

$$\dot{Q}_{cd} = -\kappa A\frac{\Delta T}{L} \tag{6}$$

where κ is the material thermal conductivity, A is the heat transfer cross-section, ΔT is the differential temperature across the heat transfer element, and L is the material thickness. Subscript *cd* accounts for conduction.

Heat exchange between PCM and heat exchanger wall occurs through convection; therefore, the following equation applies:

$$\dot{Q}_{cv} = hA\Delta T \tag{7}$$

where h represents the convection coefficient.

If two working fluids are involved in the heat transfer process:

$$\dot{Q}_{cv} = UA\frac{\Delta T_1 - \Delta T_2}{\log\frac{\Delta T_1}{\Delta T_2}} \tag{8}$$

where U is the global heat transfer coefficient. Subscripts 1 and 2 account for the two involved fluids, and *cv* for convection.

The differential temperature for every working fluid depends on the flow type, parallel or counter flow: this latter mode is more effective, reducing the heat exchange area and contact length. Likewise, the convection heat transfer mode does not apply if the PCM remains solid.

On the other hand, PV panels exchange thermal energy with the surroundings through radiation, according to:

$$\dot{Q}_{rad} = \sigma \varepsilon A_{PV} \left(T_{PV}^4 - T_{amb}^4 \right) \quad (9)$$

where σ is the Boltzmann constant, ε is the PV panel surface emissivity, A is the front area, and T is the temperature in Kelvin. Subscripts *FV* and *amb* account for PV panel and ambient, respectively.

Phase Change Material

PCMs stand out from other thermal energy absorption materials thanks to their latent heat absorption capacity. On the other hand, when solidifying, the process reverses, and thermal energy is released, facilitating heat exchange in a heat exchange cycle with water. Since each PCM has different chemical properties, it is relevant to know the conditions of the PV panels before opting for an alternative, considering its price [57].

Taking into account the purpose of using a PCM, the most relevant thermal properties when selecting one are the specific heat and enthalpy in both states, a high thermal conductivity to facilitate the exchange of thermal energy with the PV panel, and the cycle of water, and a melting point that must be at a reduced temperature or temperature range that meets the needs of the panel. Likewise, there are many physical-chemical properties to consider: little or no variation in the specific volume of the PCM in both states to reduce the complexity in sizing, chemical stability of the material to prevent irreversible changes in it and thus avoid the alteration of its thermal properties, and total reversibility in the phase change process, which can only be dependent on temperature [58].

The PCM selected in this study was paraffin wax. Paraffin is an organic substance obtained through the dewaxing of mineral oils during petroleum refining. They are known as safe materials, easy to handle, and cheap. However, they can burn to a lesser extent, usually have a low thermal conductivity, are unsuitable for plastic containers' storage, and their specific volume increases considerably during the phase change. Compared to non-paraffin organic PCMs (alcohols, glycols, fatty acids, etc.), they have lower chemical durability and higher corrosion effects but are less toxic and unstable [42]. Being organic materials, they do not have an exact melting point as water or metals would have, but rather a specific range that depends on the nature and characteristics of the PCM.

Coefficient of Performance

The coefficient of performance (COP) allows knowing the effectiveness of a thermodynamic system, generally heat pumps or refrigeration systems, in producing work regarding the energy consumed. We define COP as the ratio of energy obtained based on the supplied power from external systems [59].

Cogeneration

The cogeneration process consists of two or more energy types' generation from a single power source; in our case, solar radiation is the power supply, and electric and thermal energy are the generated energy types. In our case, electric energy generation proceeds from the photovoltaic conversion of solar radiation, while thermal energy results from the PV panel heat removal.

Cogeneration is an efficient process that uses a power source since it uses the energy losses from the principal power conversion process to generate a secondary energy type, improving the global energy conversion process. Mathematically, we define the cogeneration efficiency as:

$$\eta_{cog} = \frac{\dot{W}_{pr} + \dot{W}_{aux}}{\dot{W}_s} \quad (10)$$

where $\dot{W}$ represents the power with subscript *s* accounting for the power source and *pr* and *aux* for the principal and auxiliary energy generation type, respectively.

Compared to a single power conversion process, we have:

$$\eta_r = \frac{\eta_{cog}}{\eta_o} = 1 + \frac{\dot{W}_{aux}}{\dot{W}_{pr}} \tag{11}$$

We observe that the efficiency ratio increases with the auxiliary energy generation.

Applying the energy conservation principle:

$$\dot{W}_s = \dot{W}_{pr} + \dot{W}_{aux} + \dot{W}_L \tag{12}$$

where $\dot{W}_L$ represents the energy losses of the global process.

Combining Equations 10 and 12:

$$\eta_{cog} = 1 - \frac{\dot{W}_L}{\dot{W}_{pr} + \dot{W}_{aux} + \dot{W}_L} \tag{13}$$

The analysis of Equation 13 shows that the cogeneration process efficiency tends to be unity as the energy losses lower.

In terms of energy conservation, the efficiency ratio becomes:

$$\eta_r = \left(\frac{\dot{W}_s}{\dot{W}_s - \dot{W}_{aux} - \dot{W}_L} \right) \left(\frac{\dot{W}_{pr} + \dot{W}_{aux}}{\dot{W}_{pr} + \dot{W}_{aux} + \dot{W}_L} \right) \tag{14}$$

If energy losses tend to zero:

$$\eta_r = \frac{1}{1 - \dot{W}_{aux} / \dot{W}_s} \tag{15}$$

Analyzing Equation 15, we realize that the efficiency ratio increases with the auxiliary energy generation.

Considering the auxiliary energy generation as a fraction of the power source:

$$\eta_r = \frac{1}{1 - F} \tag{16}$$

with

$$F = \dot{W}_{aux} / \dot{W}_s \tag{17}$$

Therefore, for negligible energy losses, the cogeneration efficiency ratio evolves with auxiliary energy generation, as shown in Figure 1.

EXPERIMENTAL DEVICE AND RESULTS

The experimental device for testing consists of a 21 Wp PV panel illuminated by a solar lamp that produces variable solar radiation depending on the distance to the panel and voltage supply. The reference value is 1022 W/m^2 at maximum input voltage, 230 V, and 25 cm distance. Lower input voltages or longer distances produce solar radiation on the panel surface below 1000 W/m^2, which is out of the focus of this work. Figure 2 shows the evolution of solar radiation on the PV panel front surface for variable input voltage and distance.

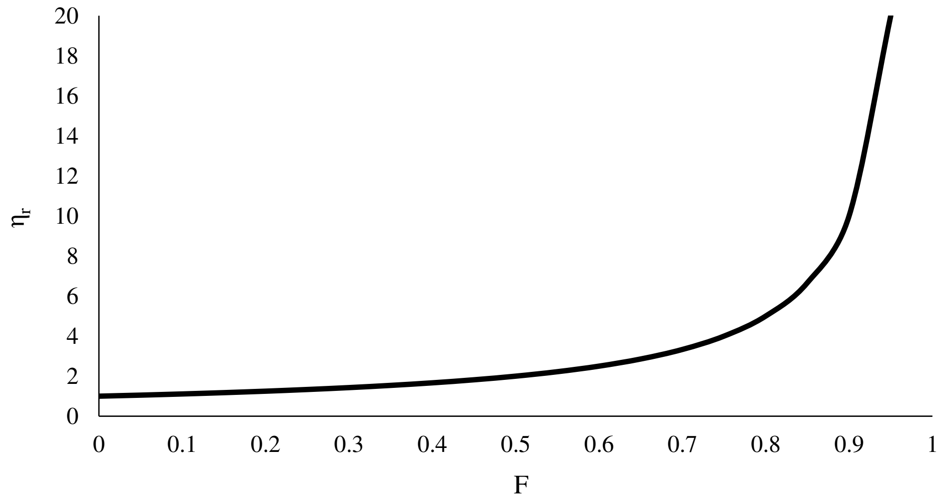

Figure 1. Cogeneration efficiency ratio versus auxiliary energy generation fraction.

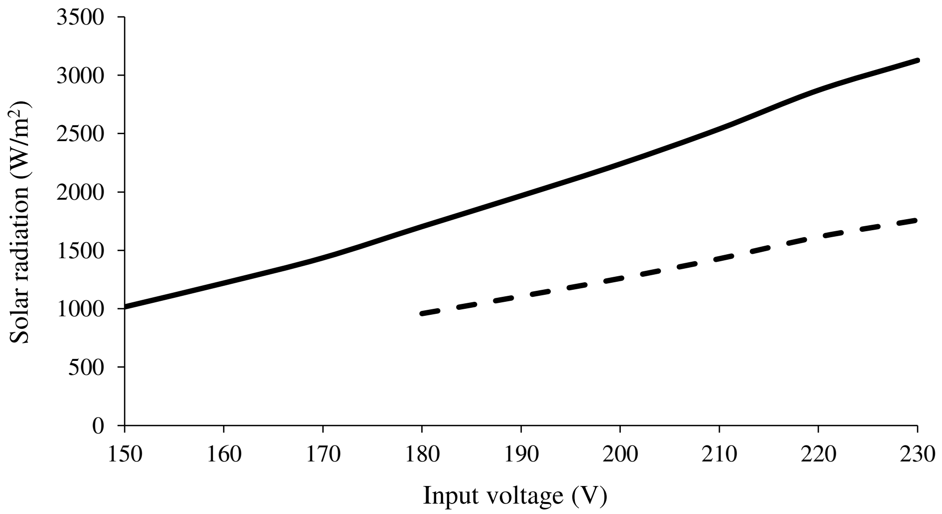

Figure 2. Solar radiation on the photovoltaic (PV) panel for variable input voltage and distance from solar radiation lamp. *Solid line: 15 cm; dashed line: 20 cm.*

We observe that we achieve a maximum solar radiation of 3128 W/m^2, corresponding to the solar concentration ratio of 3.13.

Since evaluating the system performance in the entire solar radiation range is time-consuming, we determine the system operational characteristics for a solar concentration ratio between C_x = 1 and C_x = 3.0 in 0.5 steps. C_x represents the solar concentration ratio defined as the ratio of current to standard solar radiation at sea level.

The first step is to determine the PV panel maximum power for every solar concentration ratio. For the five selected solar concentration ratios, we obtain the following results (Table 1).

Table 1. Photovoltaic (PV) panel steady state temperature for variable solar concentration.

C_x	**1.0**	**1.5**	**2.0**	**2.5**	**3.0**
T (°C) (th)	67.8	86.0	104.3	122.5	140.8
T (°C) (exp)	68.5	86.5	105.0	123.0	141.5
Deviation (%)	1.0	0.6	0.7	0.4	0.5

Correlating the experimental data to the expression developed in a previous work [60]:

$$T_{FV} = 0.0365G_{ef} + 31.289 \quad (R^2 = 0.970) \tag{18}$$

We realize the deviation is within 1%, proving the validity of the theoretical expression and the experimental results.

We manufactured the PCM device as a thick paraffin layer attached to the PV panel's rear side. The PCM is in direct contact with the PV panel, only allowing conduction heat transfer. The paraffin type used as PCM operates at a phase change temperature around 64°C, although phase change starts at 56°C and ends at 72°C. The wide temperature range for the phase change is due to the mixed organic composition, making the paraffin change phase at a variable temperature depending on every paraffin single organic compound.

Considering 64°C as the reference phase change temperature for the PCM, we notice that all solar concentration cases produce a higher PV panel steady state temperature, meaning that the PCM completely melts and is heated in the liquid phase, gaining temperature.

Heat Generation

Since we intend to operate the PV panel at a constant temperature, once the PCM melts, we have to remove the energy flow from the PV panel. Applying a thermal energy balance:

$$\dot{Q}_{PV} = \dot{Q}_{PCM} = m_{PCM} c_{PCM} \frac{\Delta T_{PCM}}{\Delta t} \tag{19}$$

Once the system reaches the steady state, the PCM does not change its temperature, and the term *ΔTPCM* becomes null, which is inconsistent with the heat transfer process; therefore, we should express the heat flow as a function of the temperature evolution of PCM during the PV panel heating. The energy balance in Equation 19 converts into:

$$m_{PCM} c_{PCM} \frac{T_{PCM,end} - T_{PCM,in}}{\Delta t} = F_R m_w c_w \frac{T_{w,out} - T_{w,in}}{\Delta t} \tag{20}$$

Or:

$$m_{PCM} c_{PCM} \frac{T_{PCM,end} - T_{PCM,in}}{\Delta t} = F_R \dot{m}_w c_w \left(T_{w,out} - T_{w,in}\right) \tag{21}$$

Equation 21 shows the energy balance between the PCM and the water flow circulating through a heat exchanger incrusted in the PCM. *m* is the mass, *c* is the specific heat, *T* is the temperature, and *t* is the time. Subscripts *PCM* and *w* account for the PCM material and water respectively, *end* and *in* correspond to the ending and initial time, respectively, of the PCM heat transfer process from PV panel to PCM, and *in* and *out* are the water inlet and outlet temperature at the heat exchanger, respectively. F_R represents the heat transfer coefficient between PCM and water at the heat exchanger and $\dot{m}_w$ is the water flow.

We determine the heat transfer coefficient for the operating conditions using a calibrated heat exchanger of the type shown in Figure 3.

The heat transfer coefficient value derives from the expression:

$$IV = m_w c_w \frac{\Delta T_w}{\Delta t} = F_R \dot{m}_f c_f \left(T_{out} - T_{in}\right) \rightarrow F_R = \frac{IV}{\dot{m}_f c_f \left(T_{out} - T_{in}\right)} \tag{22}$$

When the fluid circulates through the heat exchanger, its temperature increases, extracting heat from the tank water and reducing its temperature. If we supply electric energy to the tank water to compensate for the temperature drop, Equation 22 applies.

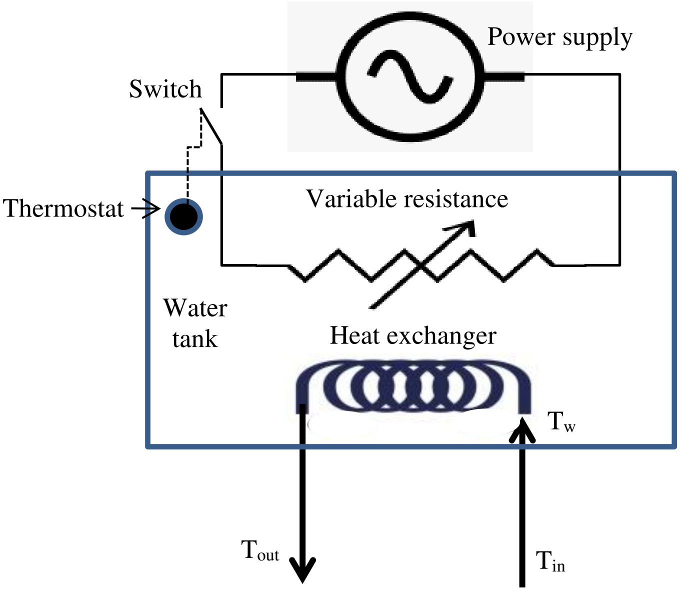

Figure 3. Heat exchange coefficient measurement device.

We design a heat exchange device similar to the PCM-heat exchanger in the experimental system with the only difference of using water in the heat exchanger container instead of a PCM. We apply a current of 1.1 A at 12 V_{DC} for a water flow of 8 l/min for a temperature gain of 25°C; using Equation 22, we have:

$$F_R = \frac{(1.1)(12)}{(1.33x10^{-4})(4180)(25)} = 0.95 \tag{23}$$

Since we measure electric voltage and current with high accuracy, the precision in determining the heat transfer coefficient depends on the accuracy determination of fluid flow, specific heat, and temperature. Applying the error theory:

$$\frac{\Delta F_R}{F_R} = \frac{(I\Delta V + V\Delta I)\left[\dot{m}_f\, c_f\,(T_{out} - T_{in})\right]^2}{(IV)^2\left[\frac{\Delta \dot{m}_f}{\dot{m}_f} c_f\,(T_{out} - T_{in}) + \frac{\Delta c_f}{c_f}\dot{m}_f\,(T_{out} - T_{in}) + \dot{m}_f\, c_f\left(\frac{\Delta T_{out}}{T_{out}} + \frac{\Delta T_{in}}{T_{in}}\right)\right]} \tag{24}$$

Applying measured and accuracy values for every magnitude results in:

$$\frac{\Delta F_R}{F_R} = \frac{\left[(1.1)(0.001) + (12)(0.001)\right]\left[(1.33x10^{-4})(4180)(25)\right]^2}{(13.2)^2\left[(0.0125)(4180)(25) + (0.001)(1.33x10^{-4})(25) + (1.33x10^{-4})(4180)(0.002 + 0.002)\right]} = 10^{-5} \tag{25}$$

The high accuracy, almost 100%, in determining the heat transfer coefficient warranties the quality of the value.

PCM tends to match PV panel temperature due to heat transfer; however, since the heat exchanger removes thermal energy from the PCM, the steady state temperature corresponds to a lower value depending on the heat exchange between PCM and water at the heat exchanger.

Because one of the goals of attaching a PCM to a PV panel is to maintain a constant temperature to operate the PV panel at constant efficiency, we regulate the water flow across the heat exchanger to keep the PCM temperature within phase change limits.

Table 2. Photovoltaic (PV) to phase change material (PCM) heat flow for variable solar concentration

C_x	1.0	1.5	2.0	2.5	3.0
ΔT (°C)	4.5	22.5	41.0	59.0	77.5
Δt (s)(x10^3)	16	11	9.5	8.5	7.0
$\dot{Q}_{PCM}$ (W)	1.77	12.89	27.19	43.73	69.75

Table 3. Phase change material (PCM) to water heat flow for variable solar concentration

C_x	1.0	1.5	2.0	2.5	3.0
$\dot{Q}_{PCM}$ (W)	1.68	12.24	25.83	41.54	66.26

Considering the PCM phase change temperature is 64°C, as mentioned before, using data from Table 1, considering the water density remains constant at 1000 kg/m^3, and applying Equation 18, we have (Table 2).

Correlating heat flow to solar concentration ratio, we obtain:

$$\dot{Q}_{PCM} = 9.1569C_x^2 - 3.2676C_x - 3.6053 \quad (R^2 = 0.9983) \tag{26}$$

Equation 26 provides the heat flow from the PV panel to PCM as a function of the solar concentration ratio.

Considering the heat transfer coefficient remains constant, the heat flow from PCM to water at the heat exchanger is as given in Table 3.

Electricity Generation

We determine the electricity generation from the photovoltaic panel for variable solar concentration ratio, measuring the output voltage and current at the maximum power point (MPP). To this goal, we connect the PV panel to a maximum power point tracking (MPPT) device and the MPPT to a continuous current power analyzer, which supplies voltage, current, and power. Table 4 shows the results for the operating solar concentration ratio.

We may determine the PV panel efficiency improvement due to the cogeneration process analyzing the combined PV output power, electric and thermal. Combining results from Tables 2 and 4, we obtain the PV output power generation for the operating solar concentration ratio (Table 5).

Since the PV panel front area is 0.1 m^2, the photovoltaic conversion efficiency is (Table 6).

Table 4. Photovoltaic (PV) maximum power generation.

C_x	1.0	1.5	2.0	2.5	3.0
P_{PV} (W)	21.6	32.4	47.0	54.4	63.0

Table 5. Global power generation.

C_x	1.0	1.5	2.0	2.5	3.0
P_{PV} (W)	23.37	45.29	74.19	98.13	132.75

Table 6. Photovoltaic (PV) efficiency.

C_x	1.0	1.5	2.0	2.5	3.0
η_{PV} (W)	0.234	0.302	0.371	0.393	0.443

Table 7. Photovoltaic (PV) efficiency improvement ratio.

C_x	1.0	1.5	2.0	2.5	3.0
r	1.113	1.438	1.766	1.869	2.107

The following equation applies:

$$\eta_{PV} = \frac{P_{out}}{C_x G S} \quad (27)$$

P_{out} is the maximum PV output power, G is the solar radiation, and S is the PV panel front area.

Analyzing data from Table 6, we observe that PV efficiency increases with solar concentration ratio due to the cogeneration process. The PV efficiency ratio evolution with solar concentration ratio, considering an efficiency reference value of 21% for standard conditions, $C_x = 1$, is as given in Table 7. The results from Table 7 show that we improved the PV efficiency by more than 100% when operating at a solar concentration ratio of $C_x = 3.0$.

If we correlate PV panel efficiency to solar concentration ratio, it results in:

$$r_{\eta_{PV}} = 0.8912 \ln C_x + 1.1037 \quad (R^2 = 0.99) \quad (28)$$

Equation 28 shows the PV panel efficiency improves with the cogeneration process in a logarithmic way with a solar concentration ratio.

Coefficient of Performance

Regarding the PV panel efficiency, the cogeneration process increases the value due to the heat generation. Applying Equations 15 and 16 and using values from Table 3, we obtain (Table 8). The correlation between COP and C_x results in a linear dependence, as shown in the following expression:

$$COP = 0.1286 C_x + 0.8901 \quad (R^2 = 0.9941) \quad (29)$$

Analyzing results from Table 8, we observe that the cogeneration process increases the global efficiency up to 28.3% for the maximum solar concentration ratio. This value, however, raises linearly with the C_x value, as shown in equation 29; extrapolating for higher concentration ratios, we obtain (Figure 4).

Table 8. Coefficient of performance (COP).

C_x	1.0	1.5	2.0	2.5	3.0
COP	1.017	1.089	1.148	1.199	1.283

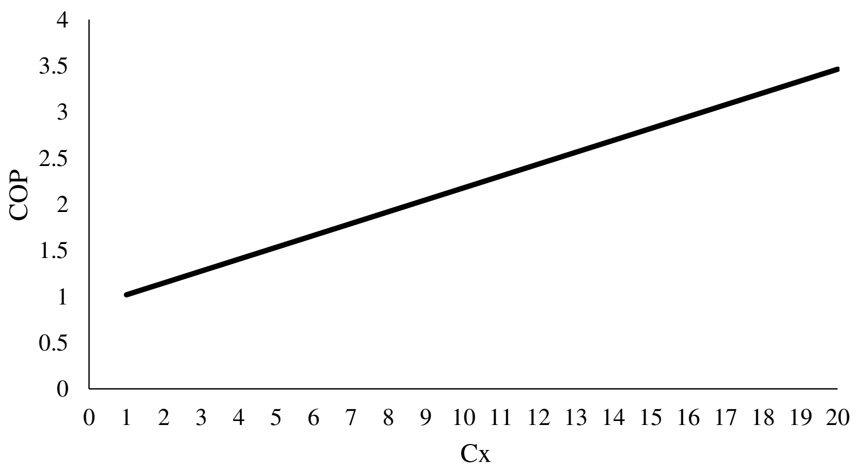

Figure 4. Evolution of the coefficient of performance (COP) for a photovoltaic–phase change material (PV-PCM) cogeneration system with solar concentration ratio.

We realize that the PV-PCM system, operating under cogeneration mode, may reach a COP close to 3.5 for a solar concentration ratio of 20; this COP value matches the heat pump system for refrigeration mode, which is one the most efficient systems in the conversion energy field.

CONCLUSION

The heat generation removal in concentrated solar radiation photovoltaic panels combined with thermal energy generation improves the PV panel efficiency and increases global energy generation. Photovoltaic panel efficiency increases up to 2.1 times for a solar concentration ratio of 3.0 when operating under cogeneration mode through an attached thermal energy generator. The PV panel efficiency ratio increase depends on the solar concentration ratio in a logarithmic way with 99% accuracy. This high correlation between PV panel efficiency and solar concentration ratio allows an accurate prediction of efficiency improvement for higher solar concentration ratios.

The cogeneration process in a hybrid PV panel-PCM-heat exchanger system increases the global power generation up to two times the electric generation at the PV panel for a solar concentration of 3.0; this value represents an effective energy gain of 107%. The thermal energy generated by removing the enthalpy excess in the PV panel depends on the solar concentration ratio through a second-degree polynomial function with 99.8% accuracy.

The hybrid system COP evolves from a minimum of 1.017 to a maximum of 1.283 within the operating range of the solar concentration ratio, $C_x = 1$ to $C_x = 3$. The COP increases linearly with the solar concentration ratio, reaching a value of 3.5 for $C_x = 20$; this COP value matches the highest efficiency of the most efficient energy conversion devices.

REFERENCES

1. Trainer T. Renewable Energy Cannot Sustain a Consumer Society. New York, NY, USA: Springer Science & Business Media; 2007.
2. Andersen O. Unintended Consequences of Renewable Energy: Problems to Be Solved. New York, NY, USA: Springer Science & Business Media; 2013.
3. Richards G, Noble B, Belcher K. Barriers to renewable energy development: a case study of large-scale wind energy in Saskatchewan, Canada. Energy Policy. 2012; 42: 691–698.
4. Toke D. Ecological modernisation, social movements and renewable energy. Environ Politics. 2011; 20 (1): 60–77.
5. Delicado A, Figueiredo E, Silva L. Community perceptions of renewable energies in Portugal: impacts on environment, landscape and local development. Energy Res Soc Sci. 2016; 13: 84–93.
6. Lamhamedi BEH, de Vries WT. An exploration of the land–(renewable) energy nexus. Land. 2022; 11 (6): 767.
7. Pasqualetti MJ. Social barriers to renewable energy landscapes. Geogr Rev. 2011; 101 (2): 201–223.
8. Sánchez-Zapata JA, Pérez-García JM, Botella F, Clavero M, Donázar JA, Carrete M, DeVault TL, Hermoso V, Losada MA, Polo MJ, Sánchez-Navarro S, Ibáñez C. Effects of renewable energy production and infrastructure on wildlife. In: Mateo R, Arroyo B, Garcia J, editors. Current Trends in Wildlife Research. Cham, Switzerland: Springer; 2016. pp. 97–123.
9. Northrup JM, Wittemyer G. Characterising the impacts of emerging energy development on wildlife, with an eye towards mitigation. Ecol Lett. 2013; 16 (1): 112–125.
10. Sayed ET, Wilberforce T, Elsaid K, Rabaia MKH, Abdelkareem MA, Chae KJ, Olabi AG. A critical review on environmental impacts of renewable energy systems and mitigation strategies: wind, hydro, biomass and geothermal. Sci Total Environ. 2021; 766: 144505.
11. Brunette CL, Byrne J, Williams CK. Resolving conflicts between renewable energy and wildlife by promoting a paradigm shift from commodity to commons-based policy. J Int Wildlife Law Policy. 2013; 16 (4): 375–397.
12. Tinsley E, Froidevaux JS, Zsebők S, Szabadi KL, Jones G. Renewable energies and biodiversity: impact of ground-mounted solar photovoltaic sites on bat activity. J Appl Ecol. 2023; 60 (9): 1752–1762.

13. Livet F. The problem of intermittency of renewable energies: solar and wind energy (No. INIS-FR--14-0410). Sauvons le Climat-SLC. 2011. Available at https://inis.iaea.org/collection/NCLCollectionStore/_Public/45/071/45071208.pdf?r=1&r=1
14. Sovacool BK. The intermittency of wind, solar, and renewable electricity generators: technical barrier or rhetorical excuse? Utilities Policy. 2009; 17 (3–4): 288–296.
15. Mlilo N, Brown J, Ahfock T. Impact of intermittent renewable energy generation penetration on the power system networks – a review. Technol Econ Smart Grids Sustain Energy. 2021; 6 (1): 25.
16. Rahimi E, Rabiee A, Aghaei J, Muttaqi KM, Nezhad AE. On the management of wind power intermittency. Renew Sustain Energy Rev. 2013; 28: 643–653.
17. Suberu MY, Mustafa MW, Bashir N. Energy storage systems for renewable energy power sector integration and mitigation of intermittency. Renew Sustain Energy Rev. 2014; 35: 499–514.
18. Kosonen I. Intermittency of Renewable Energy; Review of Current Solutions and Their Sufficiency. Bachelor’s Thesis. Lappeenranta, Finland: Lappeenranta University of Technology; 2018.
19. Barton JP, Infield DG. Energy storage and its use with intermittent renewable energy. IEEE Trans Energy Conversion. 2004; 19 (2): 441–448.
20. Rugolo J, Aziz MJ. Electricity storage for intermittent renewable sources. Energy Environ Sci. 2012; 5 (5): 7151–7160.
21. Dubey S, Sarvaiya JN, Seshadri B. Temperature dependent photovoltaic (PV) efficiency and its effect on PV production in the world – a review. Energy Procedia. 2013; 33: 311–321.
22. Rappaport P. The photovoltaic effect and its utilization. Solar Energy. 1959; 3 (4): 8–18.
23. Dupré O, Vaillon R, Green MA. Thermal Behavior of Photovoltaic Devices. Physics and Engineering. New York, NY, USA: Springer; 2017.
24. Leow WZ, Irwan YM, Safwati I, Irwanto M, Amelia AR, Syafiqah Z, Fahmi MI, Rosle N. Simulation study on photovoltaic panel temperature under different solar radiation using computational fluid dynamic method. J Phys Conf Ser. 2020; 1432: 012052. doi: 10.1088/1742-6596/1432/1/012052.
25. Muller M, Marion B, Rodriguez J. Evaluating the IEC 61215 Ed.3 NMOT procedure against the existing NOCT procedure with FV modules in a side-by-side configuration. In: 38th IEEE Photovoltaic Specialists Conference, Austin, TX, USA, June 3–8, 2012. pp. 697–702.
26. Du Y, Fell CJ, Duck B, Chen D, Liffman K, Zhang Y, Gu M, Zhu Y. Evaluation of photovoltaic panel temperature in realistic scenarios. Energy Conversion Manage. 2016; 108: 60–67.
27. Rahman MM, Hasanuzzaman M, Rahim NA. Effects of various parameters on PV-module power and efficiency. Energy Conversion Manage. 2015; 103: 348–358.
28. Amelia AR, Irwan YM, Leow WZ, Irwanto M, Safwati I, Zhafarina M. Investigation of the effect temperature on photovoltaic (PV) panel output performance. Int J Adv Sci Eng Inform Technol. 2016; 6 (5): 682–688.
29. Luque A, Hegedus S, editors. Handbook of Photovoltaic Science and Engineering. Hoboken, NJ, USA: John Wiley & Sons; 2011.
30. Kumar K, Sharma SD, Jain L. Standalone Photovoltaic (PV) Module Outdoor Testing Facility for UAE Climate. Ras al-Khaimah, United Arab Emirates: CSEM-UAE Innovation Centre LLC; 2007.
31. Grubišić-Čabo F, Nižetić S, Giuseppe Marco T. Photovoltaic panels: a review of the cooling techniques. Trans FAMENA. 2016; 40 (SI-1): 63–74.
32. Bayrak F, Oztop HF, Selimefendigil F. Experimental study for the application of different cooling techniques in photovoltaic (PV) panels. Energy Conversion Manage. 2020; 212: 112789.
33. Dwivedi P, Sudhakar K, Soni A, Solomin E, Kirpichnikova I. Advanced cooling techniques of PV modules: a state of art. Case Stud Therm Eng. 2020; 21: 100674.
34. Bahaidarah HM, Baloch AA, Gandhidasan P. Uniform cooling of photovoltaic panels: a review. Renew Sustain Energy Rev. 2016; 57: 1520–1544.
35. Zubeer SA, Mohammed HA, Ilkan M. A review of photovoltaic cells cooling techniques. E3S Web Conf. 2017; 22: 00205.

36. Sharaf M, Yousef MS, Huzayyin AS. Review of cooling techniques used to enhance the efficiency of photovoltaic power systems. Environ Sci Pollut Res. 2022; 29 (18): 26131–26159.
37. Armenta-Déu C. PV panel efficiency improvement using a hybrid PV-TEG assembly system. Int J Embed Syst Emerg Technol. 2021; 7 (2): 12–26. doi: 10.37628/jeset.v7i2.1566.
38. Armenta-Déu C, Mosquera L. Heat sink-PCM device for PV efficiency improvement. J Therm Eng Appl. 2021; 8 (2): 35–48. doi: 10.37591/jotea.v8i2.5883.
39. Ghasemian M, Sheikholeslami M, Dehghan M. Performance improvement of photovoltaic/thermal systems by using twisted tapes in the coolant tubes with different cross-section patterns. Energy. 2023; 279: 128016.
40. Khosravi K, Eisapour AH, Rahbari A, Mahdi JM, Talebizadehsardari P, Keshmiri A. Photovoltaic-thermal system combined with wavy tubes, twisted tape inserts and a novel coolant fluid: energy and exergy analysis. Eng Appl Comput Fluid Mech. 2023; 17 (1): 2208196.
41. Waqas A, Jie J. Effectiveness of phase change material for cooling of photovoltaic panel for hot climate. J Solar Energy Eng. 2018; 140 (4): 041006.
42. Khan MMA, Saidur R, Al-Sulaiman FA. A review for phase change materials (PCMs) in solar absorption refrigeration systems. Renew Sustain Energy Rev. 2017; 76: 105–137. doi: 10.1016/j.rser.2017.03.070.
43. Qu M, Tang Y, Zhang T, Li Z, Chen J. Experimental investigation on the multi-mode heat discharge process of a PCM heat exchanger during TES based reverse cycle defrosting using in cascade air source heat pumps. Appl Therm Eng. 2019; 151: 154–162.
44. Bakhshipour S, Valipour MS, Pahamli Y. Parametric analysis of domestic refrigerators using PCM heat exchanger. Int J Refrigeration. 2017; 83: 1–13.
45. Khan MIH. Conventional refrigeration systems using phase change material: a review. Int J Air-Condition Refrigeration. 2016; 24 (3): 1630007.
46. Nilsson LJ, Bauer F, Åhman M, Andersson FNG, Bataille C, de la Rue du Can S, Ericsson K, Hansen T, Johansson B, Lechtenböhmer S, van Sluisveld M, Vogl V. An industrial policy framework for transforming energy and emissions intensive industries towards zero emissions. Climate Policy. 2021; 21 (8): 1053–1065.
47. Ngoc UN, Schnitzer H. Zero emissions systems in food processing industry. WSEAS Trans Environ Dev. 2008; 4: 313–333.
48. Teke I, Ağra Ö, Atayılmaz ŞÖ, Demir H. Determining the best type of heat exchangers for heat recovery. Appl Therm Eng. 2010; 30 (6–7): 577–583.
49. Arsenyeva OP, Tovazhnyansky LL, Kapustenko PO, Khavin GL. Optimal design of plate-and-frame heat exchangers for efficient heat recovery in process industries. Energy. 2011; 36 (8): 4588–4598.
50. Morales-Ruiz S, Rigola J, Oliet C, Oliva A. Analysis and design of a drain water heat recovery storage unit based on PCM plates. Appl Energy. 2016; 179: 1006–1019.
51. Qin Z, Ji C, Low ZH, Tong W, Wu C, Duan F. Geometry effect of phase change material container on waste heat recovery enhancement. Appl Energy. 2022; 327: 120108.
52. Moldgy A, Parameshwaran R. Study on thermal energy storage properties of organic phase change material for waste heat recovery applications. Mater Today Proc. 2018; 5 (8): 16840–16848.
53. Iqbal M. An Introduction to Solar Radiation. San Diego, CA, USA: Academic Press; 1983.
54. Angulo M. Desarrollo de un Sistema Fotovoltaico de Concentración para aplicaciones de Co-Generación. Tesis de Maestría. Leon, Mexico: Centro de Investigación en óptica; 2018.
55. Markvart T, Castañer L, editors. Practical Handbook of Photovoltaics: Fundamentals and Applications. New York, NY, USA: Elsevier; 2003.
56. Incropera FP, De Witt DP. Fundamentals of Heat and Mass Transfer. 4th edition. New York, NY, USA: John Wiley & Sons; 1996.
57. Mehling H, Brütting M, Haussmann T. PCM products and their fields of application – an overview of the state in 2020/2021. J Energy Storage. 2022; 51: 104354. doi: 10.1016/j.est.2022.104354.

58. Zhang S, Feng D, Shi L, Wang L, Jin Y, Tian L, Li Z, Wang G, Zhao L, Yan Y. A review of phase change heat transfer in shape-stabilized phase change materials (ss-PCMs) based on porous supports for thermal energy storage. Renew Sustain Energy Rev. 2021; 135: 110127. . doi: 10.1016/j.rser.2020.110127.
59. Cengel YA, Boles MA. Termodinámica. 8th edition. Mexico City, Mexico: McGraw-Hill; 2015.
60. Armenta-Déu C, Mosquera L. Heat sink-PCM device for PV efficiency improvement. J Therm Eng Appl. 2021; 8 (2): 35–48. doi: 10.37591/jotea.v8i2.5883.

